Self-Assembling Nanodiscs Technology Exploration with Single-Molecule Biophysics Experimentation using Site-Specific Attachment Atomic Force Microscopy

Stephanie Elizabeth Talder
Department of Molecular, Cellular, and Developmental Biology, University of Colorado Boulder

Defense Date:
April 5th, 2022

Thesis Advisor:
Dr. Thomas Perkins, Molecular, Cellular, and Developmental Biology

Defense Committee:
Dr. Jennifer Martin: Molecular, Cellular, and Developmental Biology
Dr. Marcelo Sousa: Biochemistry

Abstract

The relationship between membrane proteins and functional cells is not yet fully understood, in large part due to the lack of knowledge about the structure and dynamics of membrane proteins. Because of the recent advancement of biotechnology, the visualization of membrane protein dynamics and energetics has progressed significantly, in large part due to nanodisc technology. Nanodiscs allow for the formation of a native environment for membrane proteins, which is essential to learning more about their structure. Atomic force microscopy (AFM) allows for the precise imaging of membrane proteins as well as the utilization of single-molecule force spectroscopy (SMFS). When completing single-molecule experimentation, it is crucial that the covalent attachment of the probe is completed, because it allows for hundreds of force-extension traces from a single molecule to be completed. Another essential aspect of site-specific attachment is passivation is necessary for unwanted interactions between the AFM cantilever tip and a single probe molecule. The focus of my senior thesis is to work with the optimization of nanodisc technology formation embedded with the membrane protein bacteriorhodopsin (bR). The bR was inserted into nanodiscs in both wild-type and c-terminal cysteine transformed to allow for site-specific labeling. The formation of nanodiscs with c-terminal cysteine bR was then labeled with DBCO-Maleimide tagging to allow for covalent connections when utilizing AFM SMFS. Altogether, this work shows a methodology for the optimization of nanodisc formation containing c-terminal cysteine bR membrane protein and warrants further investigation utilizing AFM imaging and SMFS with varying conditions of site-specific spectroscopy to target the development of protein-membrane dynamics.

Introduction

Integral Transmembrane Proteins

Membrane proteins perform vital roles in biological processes and homeostatic regulation within cells. Membrane proteins complete vital cell functions such as ATP synthesis, oxidative phosphorylation, membrane fusion, proton pumping, transport of metabolites, communication between cellular compartments, intercellular and intracellular signaling, and biosynthesis[17]. Their structure is composed of monomeric amino acids bound by peptide bonds creating polypeptides. These monomers contain a similar composition with the variation of a single side chain (R-group). The R-group allows for variation of properties: hydrophobic, charged (positive or negative), and/or polar. These properties drive their structure and association through covalent bonds, non-covalent bonds, ionic bonds, and hydrophobic/hydrophilic interactions[18]. Proteins' functions are dictated by their structure; thus, a complete understanding of their structure can allow for disease regulation and health applications. Integral transmembrane proteins lie within the phospholipid membrane bilayer and allow for connection from the extracellular space to the cytosol of cells[18]. These proteins have hydrophobic amino acid portions that associate with the lipid tails of the phospholipids allowing for integration into the membrane. Understanding how membrane proteins function and their protein stability are crucial in pharmaceutical applications. Membrane protein dynamics and stability are key points of focus for research due to them being a target for 60% of medications[21].

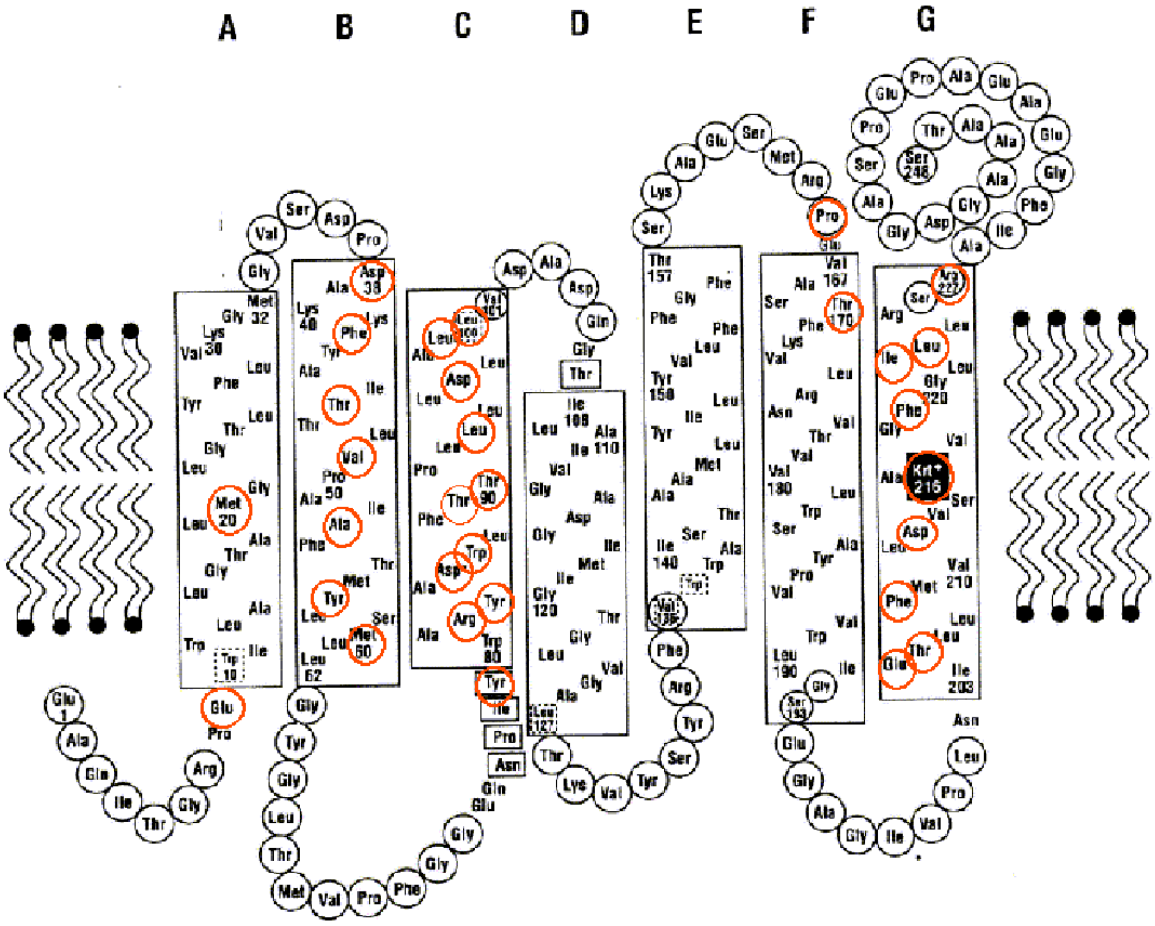

Figure 1: Integral transmembrane protein bacteriorhodopsin- wild type: Depicted is the amino acid sequence of bacteriorhodopsin, a membrane protein that exists in the intermembrane and peripheral membrane space of *Halobacterium salinarum*. The model is the secondary structure model of bR based on electron cryo-microscopy showing the helical membrane-embedded shown in the box. The red circle outlines the residues that lie within the proton channel. Adapted from Protein Science[3].

Traditional Reconstitution Methods

Membrane proteins' structure is highly dependent on the association to their native lipid bilayer which leads to denaturation and therefore altered activity following removal from this native environment, making them challenging to study in a laboratory in vitro experiment[4]. The typical methods used in membrane protein research rely on detergent micelles which have a variety of properties, including ionic, bile acid salt, nonionic (ex. dodecyldimethyl-*N*-amineoxide, *n*-octyl-β-d-glucopyranoside, *n*-dodecyl-β-d-maltoside), zwitterionic, tripod, and amphipols[19]. These detergent micelles cause protein denaturation and deactivation, making them non-ideal for use in studying proteins.

The other reconstitution methods that are traditional for membrane protein isolation are lipid-detergent micelles methods such as detergent solubilization, dilution, organic solvent-mediated, sonication, and bicelles[14]. The issues that arise from these methods are the improper refolding of proteins, fragile or small liposomes, and deactivation[7]. Typical methods require removal from the native lipid bilayer leading again to problematic deactivation[7].

Bacteriorhodopsin Membrane Protein

Wild-Type Bacteriorhodopsin

Bacteriorhodopsin (bR) is a model membrane protein that functions as a proton pump in the archaea *Halobacterium salinarum*[6]. It contains seven transmembrane helical regions forming a trimer in the active state leading to the functionality of proton translocation[10]. Previous research on bR shows that many ion pumps share common principles. Proton translocation is completed through the Schiff base and two aspartate residues, Asp 85 and Asp 96. The Schiff base donates a proton to Asp 85 following photoisomerization from all-*trans* to 13-*cis*. Then the re-protonation

of the Schiff base occurs from Asp 96. Due to these internal proton translocations, the proton is released into the extracellular space from the cytoplasmic surface[3]. Proton translocation between the Schiff base, Asp 85, and Asp 96 is recognized as equivalent to other ion pumps[2]. bR is frequently used as a model protein due to the 2D-lattice structure within its native environment, allowing for a higher density of proteins for experimentation (Figure 1).

Nanodisc Technology

Nanodiscs are assembled using an amphipathic helical protein referred to as a membrane scaffolding protein (MSP) surrounding a phospholipid membrane[24]. This phospholipid membrane can be composed of native lipids from the membrane proteins environment or made from synthetic lipids[20]. This allows for an effective membrane mimicking system that provides minimum alteration to the membrane protein's structure[27 28]. The strong interactions between the MSPs and lipids within nanodiscs provide higher stability and a better-defined structure than traditional self-assembled systems such as liposomes[7]. Nanodiscs can be readily fixed to a variety of surfaces, and are homogenous and monodisperse, allowing for single-molecule studies without the loss of function[7].

Atomic Force Microscopy

Atomic Force Microscopy Used to Study Membrane Protein Dynamics

Atomic force microscopy (AFM) is a powerful technique used to image nearly any surface including composites, ceramics, polymers, biological samples, and glass[5]. AFM uses a cantilever tip to scan over the desired surface to measure the deflection of the cantilever allowing for imaging on the surface[11]. This deflection is measured using a laser deflecting off the

cantilever and detected by a quadrant photodiode. AFM also has the power to measure forces between the sample and tip when coming into contact and pulling away from the sample, known as single-molecule force spectroscopy (SMFS)[18 28]. This allows for important aspects of protein dynamics and energetics of protein folding to be measured by pulling a protein out of the membrane[7]. The verification of this is what will be analyzed with this thesis project.

AFM Site-Specific Attachment using Maleimide-DBCO Labeling

Traditional AFM-based SMFS experimentation utilizes nonspecific attachment on both the surface and cantilever tip[14]. Such non-specific attachment leads to a significantly lower attachment rate causing sticking to the surface leading to lower data quality[13]. The attachment of a functional group or molecule onto the surface of an AFM tip allows for the specific attachment of complementary targets on sample surfaces[13]. The use of specific attachment leads to several advantages over traditional methods, such as making it significantly easier to discriminate and interpret protein unfolding when compared to non-specific attachment and there is approximately a 75-fold increase in the acquisition rate of high-quality protein unfolding data[24 9].

Malemide-dibenzocyclooctyne (DBCO) labeling is a copper-free click chemistry reagent that allows for completing labeling without the addition of metals creating a decrease in interference with AFM-based SMFS[26]. This is able to form a covalent bond with azide allowing for long-term experiments with repeated unfolding and refolding. Maleimide readily reacts with cysteine residues which are easily integrated into proteins. This allows for labeling to be much easier when completing SMFS, generating an ability to create specific bonding with the cantilever tip containing Saline-PEG-Azide.

Silane-PEG-Azide Labeling of Cantilever Tip

The cantilevers were functionalized using silane and azide with PEG as a spacer. The silane reacts with glass or the cantilever tip (silane nitride) by interacting with the activated oxygens on the surface. The azide is able to form covalent bonds with DBCO tags[26].

Introduction of C-terminal Cysteine to Bacteriorhodopsin (bR NΔ8)

To characterize bR using site-specific attachment atomic force microscopy (AFM), there must be a mutation completed on the c-terminal end of the membrane protein[15]. The mutation will allow for labeling which allows for site-specific covalent attachments with the cantilever when completing pulling experiments[25] (Figure 2). A transformation was completed using a plasmid insertion into the archaea. The plasmid contained site-directed mutagenesis which is expressed in the wild-type protein membrane.

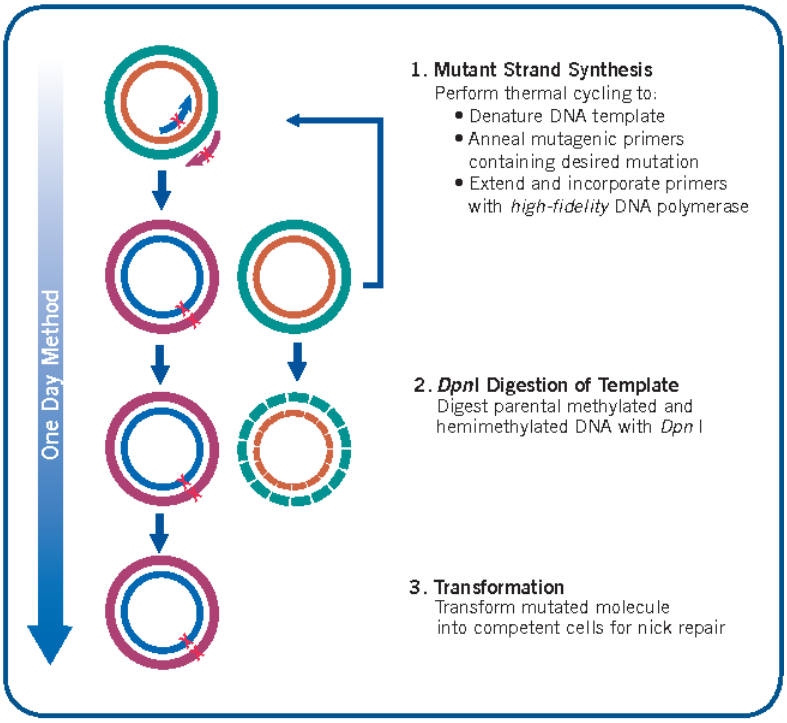

Figure 2: General diagram indicating the transformation completed within this experiment of the plasmid containing site-directed mutagenesis for future experimentation utilizing AFM-based SMFS. Adapted from Agilent Technologies[22].

Specific Aims

Hypothesis 1: Validation that the membrane protein bacteriorhodopsin from *Halobacterium salinarum* can be transferred into nanodiscs while maintaining its native lipid environment.

Aim 1: My first aim is to optimize the formation of nanodisc technology containing both wild-type and c-terminal cysteine labeled bacteriorhodopsin with the native lipid environment. To test this, we measured the yield of the reactions and optimized the reactions based on the yield of the reactants. This aim was completed by utilizing the initially published protocol from "Highly Efficient Transfer of 7TM Membrane Protein from Native Membrane to Covalently Circularized Nanodisc"[12].

Hypothesis 2: Nanodiscs and site-specific attachment facilitate the collection of high-quality force spectroscopy data by AFM.

Aim 2: My second aim is to perform initial AFM experiments on bacteriorhodopsin embedded within the nanodiscs, including both imaging and single-molecule force spectroscopy (SMFS). To test this, we collected SMFS data in the form of force-extension curves and looked into our ability to produce high-quality data. First, we created a site-specific label on the bR, allowing for an attachment within a specific section. Next, we measured the pulling force of the c-terminal cysteine bR membrane protein on an AFM cantilever.

Methods and Materials

Initial Wild-Type Bacteriorhodopsin Grow-Up from Halobacterium salinarum

Establish a liquid culture from a frozen stock

The *Halobacterium salinarum* was purchased from James Bowie's Laboratory at UCLA. To establish a colony, a tip stab was taken from the *Halobacterium salinarum* frozen stock from the -80°C freezer. The tip was placed into 10mL of complex media ((CM) 250g of NaCl, 20g of $MgSO_4$ * 7 H_2O, 3g of trisodium citrate 2 H_2O, 2g of KCl, 5g of Bacto tryptone, and 3g of Difco yeast extract (pH = 5.9)) in a sterile culture tube. The culture was then allowed to grow for 2 days at 37°C on a shaker. Then we added 1 mL of this culture to 9 mL of CM with 12.5 µL of mevinolin (4 mg/mL) stock. This was placed onto the shaker rotating at 1000g/3 minutes at 37°C for seven to ten days until the media was slightly cloudy.

Scale-up to a 1L culture

To scale up the growth of the *Halobacterium salinarum*, 4mL of the culture was placed into 1 L of rich media ((RM): 250g NaCl, 20g of $MgSO_4$ * 7 H_2O, 3g trisodium citrate * 2 H_2O, 2g KCl, and 10g Oxoid Peptone L37) without mevinolin in a 2L flask. We then placed this sample at 37°C under a full spectrum LED light (5000K, 163mA, 60Hz) for five days with shaking.

Prep harvest bacteria and start purification

Samples of the cloudy mixture of bacteria were poured into two 250 mL centrifuge tubes and spun down at 8000 rpm for 25 minutes at 4°C. The solution of supernatant is poured out,

autoclaved, and discarded. The pellet left behind was purple at the bottom of the centrifuge tube, then another 250 mL of the sample was added to the same centrifuge tube and the steps above were completed until all bacteria were grown-up. The pellet was resuspended in 1 mL of pre-lysis buffer (4M NaCl and 25 mM Tris-HCl, pH = 6.8), then transferred to a 15 mL conical tube. The sample was then frozen at -20°C.

Cell Lysis

The bacteria were thawed at room temperature in water to prepare for dialysis. Dialysis tubing with 25mm x 10-inch dimensions (12000-14000 MWCO) was washed 3 times using Ultrapure water and clipped at one end. The lysate was carefully introduced into the open side of the dialysis tubing and then clamped with another dialysis tubing clip. The tubing was placed into a 2L beaker on a stir plate containing 0.1M NaCl at 4°C and allowed to dialyze twice for an hour each. The sample was then removed from the beaker and tubing into a 15 mL conical tube.

Preparing the Purification bR

The samples of bR are poured into the 64 mL ultra-centrifuge tube and topped off with cold 0.1M NaCl. This sample is then spun in a Ty 45Ti fixed angle rotor in the Stowell lab ultra-centrifuge at 20000 rpm for 30 minutes at 4°C. Following the spin, a purple pellet was left at the bottom of the centrifuge tube with a brownish pellet at the center. This brown pellet is cell debris, DNA, and other waste products. The supernatant was poured out of this solution quickly leaving the pellet at the bottom of the centrifuge tube. We resuspended the purple pellet using 3 mL of cold 0.1M NaCl and transferred it to another 64 mL ultra-centrifuge tube, which was topped with 60 mL of 0.1M NaCl 3 times completing the same steps as stated. As each spin was

completed, the brown pellet decreased significantly each spin allowing for decreasing waste within the sample.

Sucrose Gradient Purification

To create the sucrose gradient needed for the final purification, 60%, 50%, and 30% sucrose were layered into a 64 ml ultracentrifuge tube. 170 µL of bR was pipetted onto the surface of the sucrose gradient and balanced. The sample was spun at 23,000 rpm at 17°C for 17 hours with slow acceleration and no braking. These samples were separated and the upper layer concentration was measured (176.5 µM), aliquoted into 50 ml samples, and stored in a -80°C freezer (Figure 5).

Transformation of bR-WT from Halobacterium salinarum to C-Terminal Cysteine bR NΔ8

Transformation Using Plasmid Containing C-Terminal Cysteine Variant of bR

For transformation, 10 ml of CM (without mevinolin) was inoculated into a 150 mm x 20 mm glass culture tube with a sterile pipette tip stabbed into frozen glycerol stock (from a -80°C freezer) *Halobacterium salinarum*. The specific primers that were used in the transformation using a plasmid were used to change terminal amino acid serine to cysteine at position 248 in bR (S261C): site-directed mutagenesis-forward GCGGCCGCGACCTGCGACTGATCGCACACG and site-directed mutagenesis-reverse CGTGTGCGATCAGTCGCAGGTCGCGGCCGC[2]. This was grown for 5 days at 37°C until the culture was slightly cloudy. This culture was split into three 10 ml cultures of CM and allowed to grow until moderately cloudy. From cultures, 10 ml was placed into 15 ml conical tubes and spun at 3000 rpm for 10 minutes at 25°C. The supernatant was discarded and the residual pellet remained. To this conical tube, 1 ml of

Spheroplasting solution (50mM Tris-HCl (pH=8.75), 2M NaCl, 27 mM KCl, sucrose 15% w/v) was mixed with the pellet with gentle continuous pipetting. Into a sterile 2 ml tube, the following solutions were added in the following order: 10 µL of EDTA/Spheroplasting solution (50mM Tris-HCl (pH=8.75), 0.5M EDTA, 27mM KCl, 2M NaCl, sucrose 15% w/v, and water), 200 µL of resuspended cells in Spheroplasting solution, and 15 µL of DNA (NΔ8 plasmid variant from Bowie Lab in UCLA) with gentle pipetting (the DNA is prepared with 1.5x Spheroplasting solution and DNA 1 ng/µL to induce mutation and Dpnl digestion (Table 1)). Following 5 minutes of incubation, 225 µL of PEG/unbuffered Spheroplasting solution (50mM Tris-HCl (pH=8.75), 0.5M EDTA (MW 292.2), 27mM KCl, 2M NaCl, sucrose 15% w/v, and water) was added to the sample. This tube was then inverted 20 times quickly to mix the solutions and allowed to sit for 20 minutes at 25°C. Following the incubation, 5 ml of CM/sucrose-containing bacteria was added to a 15 ml sterile conical tube. This was spun at 4000 rpm (2400 g) for 15 minutes at 25°C. The supernatant was discarded. The remaining liquid within the conical tube following the spin was flicked gently to resuspend the pellet streak adhering to the tube back into the CM. 2 ml CM/sucrose was added to a 2 ml tube to resuspend the pelleted archaea then transferred into a sterile bacterial 150 mm x 20 mm glass culture tube containing 8 ml of CM/sucrose. This solution was then placed onto a shaker for 48-72 hours at 37°C to allow for the growth of Mevinolin-resistant bacteria[2].

C-Terminal Cysteine Amplification of Plasmid with bR NΔ8 Mutation

Following incubation on the shaker, the solution was poured into a 15 ml conical tube and spun at 3000-4000 rpm for 20 minutes at 25°C. All the supernatant was discarded except 250 µL, which allowed for the pellet to resuspend giving a cloudy liquid. 100 µL of these cells were

then plated onto a CM-Agar-Mevinolin plate (Mevinolin at 4μg/ml). The plate was placed into a Ziploc bag with slight ventilation and incubated at 37°C. It was given 3 days to show the presence of a colony and those present were marked then allowed to incubate for another 12 days to increase possible colony growth. The plates were then allowed to sit at 25°C for 2 months which allowed for the colonies to be visualized but deter salt crystallization on the CM-Agar plate. A microscope was used to visualize and identify the turbid colony chosen and then picked with a sterile 20 μL tip. This colony was grown in 10 ml of CM+Mevinolin for 14 days until the culture was very cloudy then stored in a frozen glycerol stock at -80°C. Steps completed were according to initial bR-WT growth with several deviations. The volume grown in RM was 2L instead of 1L. This preparation was grown for two weeks rather than 5 days to maximize yield. The RM contained mevinolin to select for only mevinolin-resistant bR.

Freezing Cultures

By using frozen glycerol stock, the culture can be kept at its prime state because the purple-producing bacteria get lost within each passage. The samples were stored in sterile cryotubes with 250 μL 80% glycerol with 750 μL of *Halobacterium salinarum* NΔ8 clonal transformed culture. The bacteria could be activated by using a pick from a sterile pipette tip and CM+Mevinolin.

Covalent Circularization of Membrane Scaffolding Protein

With recent advances in nanodisc research and technology, the use of covalently circularized Membrane Scaffolding Proteins (MSPs) has been shown to improve stability and yield[8]. These MSPs are tagged with two His-tags: one associated with the TEV site and one with

the sortase site using an evolved version of sortase A, eSrtA. This evolved to have a higher activity and faster kinetics[8]. After circularization, both His-tags should be removed due to the cleavage activity of sortase. These are added to the protein before circularization to complete verification that the circularization was complete - if it was not complete, then a His-tag would remain. The initial step in circularization involves the addition of the TEV protease, which recognizes and cleaves the signal sequence ENLYFQG, leaving a terminal glycine. The terminal glycine that is present will be recognized by the sortase (eSrt) enzyme, covalently linking it to the eSrt-site LPETG (Figure 3). Following this, Ni-NTA is added to the solution to remove the remaining enzymes and any MSP that was not circularized[3]. The circular MSP-11 in 50 mM Tris-HCl, and 150 mM NaCl, was aliquoted in 20 µL aliquot and stored at -80℃ until needed.

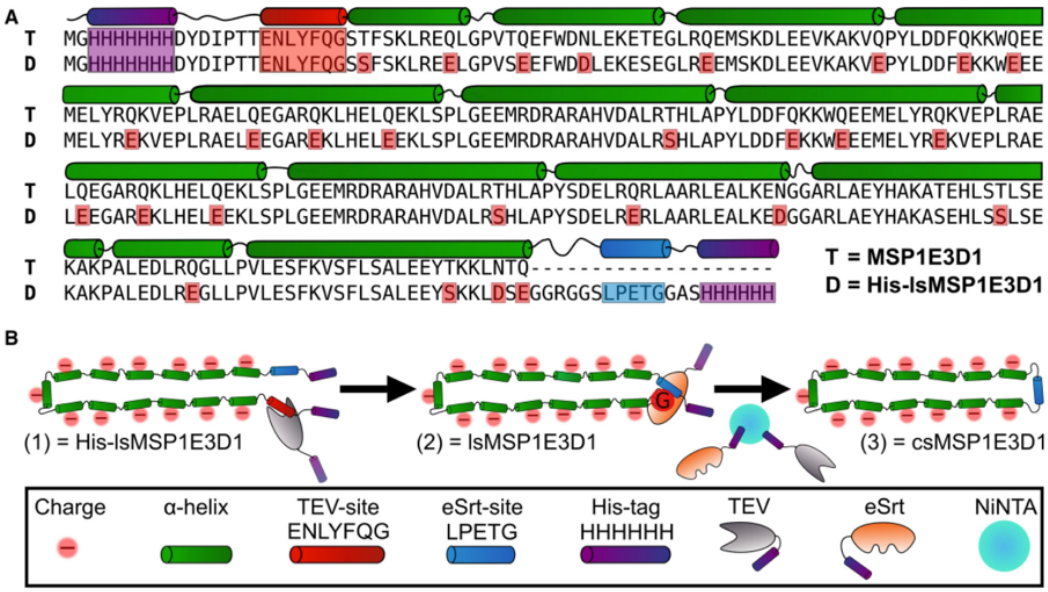

Figure 3: Covalent circularization of MSP using the TEV and sortase reaction cleaving the poly-His tag. Adapted from Johansen, N. T. et al., 2019[8].

Nanodisc Self-Assembly

In a method adapted from the "Highly Efficient Transfer of 7TM Membrane Protein from Native Membrane to Covalently Circularized Nanodisc" protocol, self-assembly of nanodiscs is achieved using the addition of 50μL bR (25μM), 246.61μL NaCl (2.5M), 8.82μL Tris-Buffer/EDTA (0.5mM), and 18.78μL MSP-11[12]. Following the resuspension, 8.33μL of Triton X-100 detergent was added to the solution to increase the miscibility of the protein into the circularized MSP-11 lipid membrane (Figure 4). Following 10 minutes of incubation at 25°C, the detergent was removed from the solution using 999μL of BioBeads equilibrated in water. The BioBead mixture was incubated at 4°C for 24 hours (Tables 2-5).

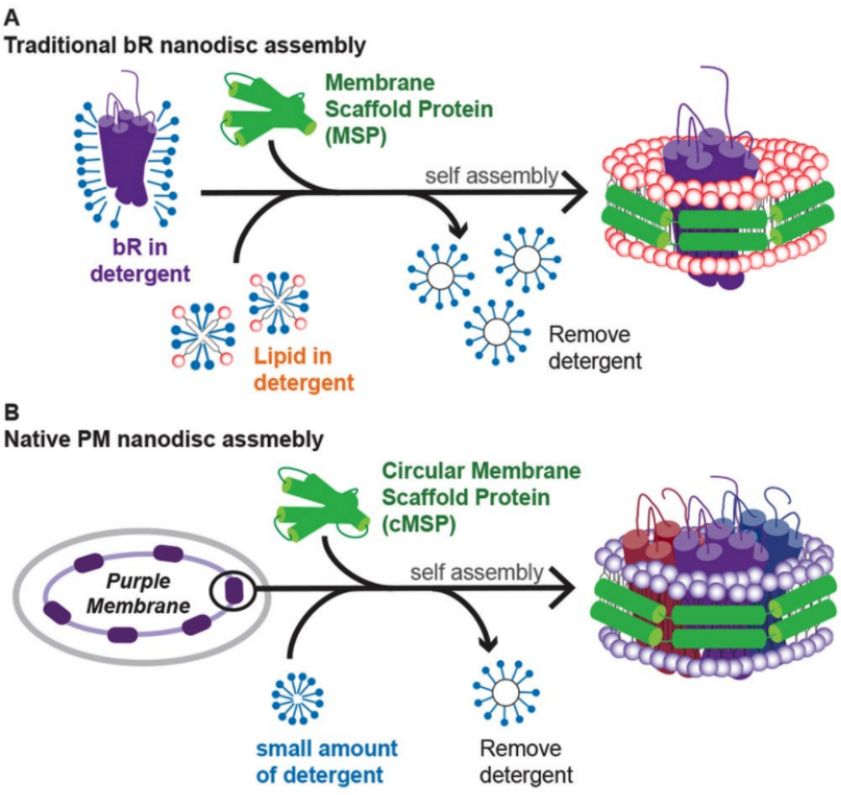

Figure 4: Assembly of nanodiscs using bR and detergent using both traditional and native phospholipid membrane assembly. (A) Traditional preparations of nanodisc assembly use lipids in detergent for the lipid bilayer. (B) Native phospholipids from membrane protein bR are used for nanodisc assembly. Adapted from Johansen, N. T. et al., 2019[8].

Dynamic Light Scattering

Following the preparation of nanodisc samples WT and c-terminal cysteine variant, the samples were transferred into new tubes to allow for separation from the BioBeads. These samples were spun in a microcentrifuge for 10 minutes at 21,000 RCF. Following the spin, both samples were diluted at concentrations in 20 mM Tris pH = 8.0, 150 mM NaCl: 1:10x, 1:100x, 1:1000x. 6µL of the samples were measured using a Punk DLS held by a Bladecell™ to measure

the successful presence of nanodiscs. The solution was set to measure with a HEPES buffer solution with 10 runs at 10 seconds of acquisition time (Figure 7).

Gel Electrophoresis Verification of Circularized MSP-11 and Maleimide-Azide Labeling

A 12% SDS PAGE protein gel using PageRuler™ Plus Pre-stained Protein Ladder was used to verify the accuracy of the circulation of the MSP-11 and the maleimide-azide labeling. The gel stain contained 200 mg Coomassie Brilliant Blue R-250, 50% methanol, deionized water, and 10% acetic acid.

Nanodrop Used to Measure all Concentrations

For measuring the concentrations of solutions, UV-Vis Spectrophotometer ND 2000C was used with 1.5 μL droplets placed onto the pedestal sample holder. Nanodisc concentration was calculated at 280 nm and bR was located at 560 nm based on previously reported values.[1]

Fast Protein Liquid Chromatography (FPLC)

FPLC was used to ensure that the nanodiscs contain active bR. To do so, we monitored the elution at 280 nm to measure total protein presence (for both bR and MSP-11) and 560 nm for active and properly folded bR. 500 μL of the nanodisc sample was loaded onto the column that was equilibrated with 25 mM TRIS and 150 mM NaCl (FPLC was completed to purify using a Superdex 200 10/300 GL from Cytiva at 0.5 mL/minute. The absorption spectra that were collected were not very clear because the UV unit of the FPLC began to fail (Figure 9).

Transmission Electron Microscopy (TEM) Used to Image Nanodiscs

TEM was completed using Electron Microscopy Sciences – CF200-CU with a carbon support film 200 mesh. The metal holder was placed into a glow discharger, loaded with the carbon side up, then the preset settings 15A with 60-second cycles lasting 5 minutes. Then using a radioactive bench, on a semi-large piece of parafilm, 8 droplets of water were placed. For each sample, 8 μL of the sample was used and deposited on the support film for 2 minutes. The extra liquid was wicked away then 3 water washes were complete with ~10 seconds/droplet. Finally, ~8 μL of UA stain was deposited 3 times for 15 seconds each then dried out.

DBCO-Maleimide Reaction on C-Terminal Cysteine Variant Nanodiscs

Site-specific attachment when completing AFM experiments requires a functionalization of the nanodisc c-terminal cysteine bR using a covalent link to a maleimide reagent. Nanodisc solution was concentrated using a 10K Millipore Filter Unit™ spun at 14,000 RCF for 4 minutes. The remaining sample contained in the filter was spun inverted at 1,000 for 2 minutes into 2 mL Epitube. Buffer exchange was completed with Zeba™ Spin Desalting Columns to replace DTT with TCEP to remove reactivity with the reagent containing a thiol group at concentrations: 150 mM NaCl, 5 mM EDTA, 1 mM TCEP, and 25 mM Tris at pH = 6.8. Following the buffer exchange, 15 mM dibenzocyclooctyne DBCO) dissolved in dimethylsulfoxide (DMSO) was combined with the sample. We aimed for 100% labeling of DBCO-Maleimide on the sample, so a 10x:1x concentration was used in this preparation of DBCO-Maleimide nanodiscs. Following the addition of DBCO to the sample, the sample was incubated at 4°C overnight.

Buffer exchange was used to remove unreacted labels from the nanodiscs. This was performed using 300 mM KCl (pH = 8) and 20 mM TRIS using a Zeba™ Spin Column. A 300 µL buffer exchange was completed twice and spun at 1 minute at 1500 RCF. Then 300µL of the exchange buffer was added to the column and spun at the same conditions four more times to ensure a full buffer exchange. The sample was added to the column along with 15 µL of buffer and spun for 2 minutes at 1500 RCF.

Silane-PEG-Azide Reaction with DBCO Labeled Nanodiscs

Following the removal of the excess label, 20 µL of DBCO labeled nanodiscs was added to 50 µL of 29 mM Silane-PEG-Azide dissolved in 20 mM TRIS (pH = 7.2) and 150 mM NaCl buffer. This solution was allowed to incubate at room temperature for 30 minutes before the product of this reaction was verified using a protein gel to determine whether the Silane-PEG-Azide caused a shift (Figure 10).

AFM Sample Preparation

Steel AFM specimen discs 15 mm in diameter were prepared for each sample covered in Teflon to prevent rusting caused by the buffer. Mica discs were cleaved along the layers using Scotch tape to create an atomically flat surface for even deposition of nanodisc solution. Following the cleavage, potassium cations localize on either side leaving a negative charge on both sides of the disc. To maintain stability, 2-part epoxy was used to secure the mica disc to the steel specimen disc. Silicone holders were applied to the surface of the mica to reduce the surface areas needing to be converted from 60 µL to 9 µL to reduce sample waste. Silicone holder holes are marked with Sharpie on the back of the sample to indicate where the sample is

located following removal of the holder. The deposition buffer used possessed a high salt content allowing for disruption of negatively charged surface to allow for proper deposition of a sample that contained 300 mM KCl (pH = 8) and 20 mM Tris. Nanodiscs were diluted to 1 μM then 9 μL was deposited onto the surface for 10 minutes. Following the deposition, 5 consecutive washes of 200 μL were completed using the deposition buffer without allowing the surface to dry out.

AFM Pulling Experimental Set-up

AFM experiments were completed using an Asylum Cypher ES AFM. The cantilever used was an Olympus-40 cantilever functionalized with Silane-PEG-Azide. The sensitivity used was discovered using the thermal method (below) by contacting the cantilever with the surface. The cantilever that was used in this experiment was measured previously in this laboratory's research at 8 pN/nm. A force-extension plot curve acquisition was completed by bringing the cantilever into contact with the surface at a velocity of 1 μm/second. The data was measured at 50 kHz but for presentation and clarity smoothed to 5 kHz. In order to reduce the non-specific attachment that occurs, the tip was pushed to the surface at 100 pN in order to promote non-specific attachment (Figure 12: a-d). The surfaces were activated using UV radiation using silane-PEG functionalization in toluene which allows for the production of maleimide-derived AFM tips. The sample was run in the deposition buffer of 300 mM KCl and 20 mM TRIS (pH = 8) at 25℃ (Figure 12: a-d).

The pulling was set up using a raster scan with 5 approaches to the surface at each location. The probing spots were separated by 1.25 microns on the grid. By bringing the tip down to the surface to come into contact, then when the sample attaches, it will start applying

force depending on how far the tip is from the surface. With SMFS, everything happens extremely close to the surface so the unfolding of the membrane protein out of the membrane is immediate. Every time the force drops, a portion of the membrane protein has unfolded, reducing the strain that is being put on the cantilever tip. This change in force allows for modeling using the wormlike chain model to measure how long the portion that has been unfolded. This data allowed for the length to be measured of bR to be pulled out of the membrane and to connect this data back to the protein structure.

AFM Imaging Experimental Set-up

The surface used containing the nanodiscs was prepared the same as the protocol above for the pulling experiment but washed with 200 μL an additional three times. An Olympus-40 cantilever was used for imaging using Tapping Mode. Imaging was complete from 500 nm by 500 nm, sensitivity was set to 41 nm/V, and the amplitude was 0.5V.

AFM Data Analysis Using The Wormlike Chain Model Methodology

When completing AFM-based SMFS, the wormlike chain model (WLC) was used to fit the contour length to the data. The contour length allows for the ability to measure how large the protein is that is being unfolded through the measuring of rupture forces. A fixed persistent length of 0.4 nm was used in this analysis. We are comparing the data obtained to the known literature length of unfolding bR[30].

Wormlike Chain Model Equation:

$$F = \frac{k_b * T}{P} * \left(\frac{1}{\left(1 - \frac{x}{L_0}\right)^2} \right)$$

L_0 = Contour length

x = Extension

k_b = Boltzmann constant

T = Temperature

F = Force

P = Persistence length

K_0 = Enthalpic compliance material parameter

Representative Results

Aim One:

Bacteriorhodopsin verification of grow-up and transformation of c-terminal cysteine

Due to the difficulties completing experiments on membrane proteins within their native environment, we began this project with the intention of verifying from the literature the formation of nanodisc technology containing c-terminal cysteine bR. To do this, we initially worked to grow up and purify a large culture of bR. Following this successful growth, we completed a plasmid transformation allowing for the bR to be labeled with a c-terminal cysteine. Following growth, a sucrose gradient was completed to purify the transformed bR (Figure 5). The intention behind this was to complete future experiments following nanodisc formation using site-specific AFM imaging and pulling. As expected, the bR transformation was successful allowing for the ability to complete membrane-embedded nanodiscs.

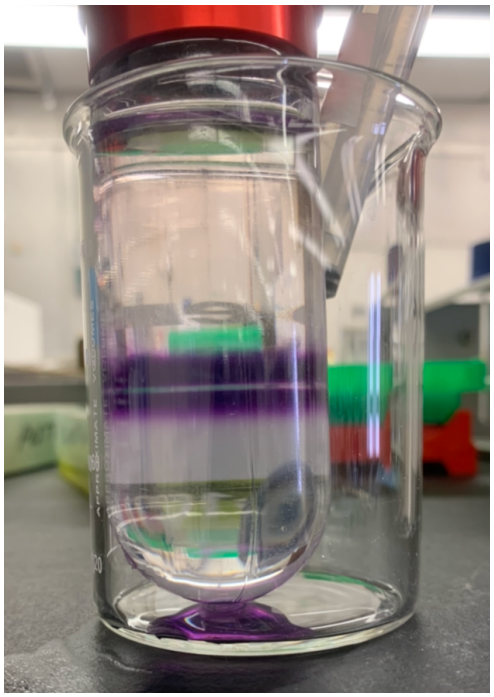

Figure 5: Successful purification of bR-WT using sucrose gradient. Two different bands indicate bR protein purification of two separate molecular weights.

Covalent circularization of MSP-11 using Sortase-TEV reaction

Following the completion of covalent circularization of MSP-11, the concentration measured was 14.4 μM using a NanoDrop. A protein SDS-PAGE gel electrophoresis was completed to verify the circularization completion. Following the circularization of MSP-11, a shift down was observed when comparing to the linear MSP-11. This validates the successful completion of ciruclairation using the TEV-Sortase reaction (Figure 6).

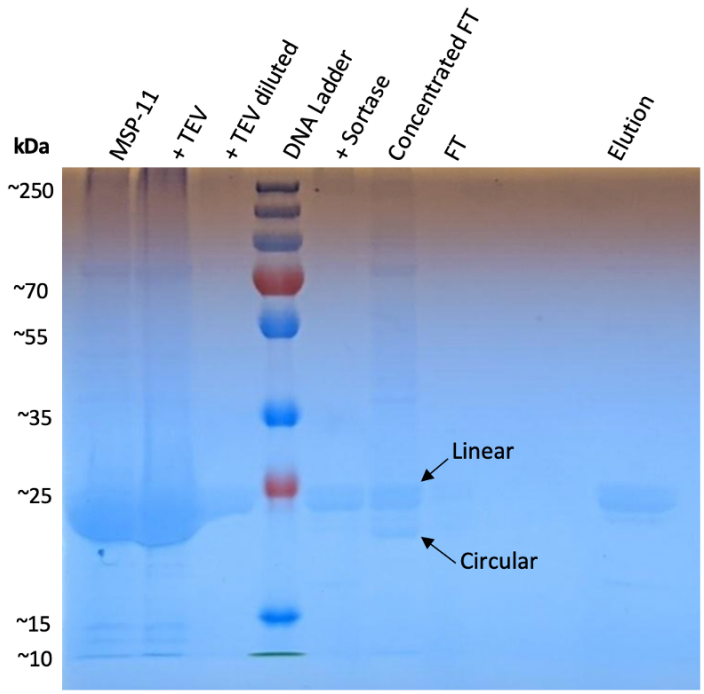

Figure 6: SDS-PAGE verification gel electrophoresis of TEV-Sortase covalent circularization of MSP-11. Circularization of MSP-11 is expected to have a lower kDa than linear MSP-11 on SDS-Page gel electrophoresis.

Validation that Bacteriorhodopsin can be transferred to nanodiscs while maintaining their native lipid environment

Successful nanodisc formation verification using DLS

When completing the DLS for the nanodisc preparation containing c-terminal cysteine bR, the diameter was observed to be 12.55 nm which matches that of which was expected. The expected size of circulaized MSP-11 is 12 nm, so the DLS validates that a high portion of the sample contains nanodiscs. There is a small peak following the main peak which shows that larger objects are within the solution such as protein aggregates (Figure 7).

Peak #	Mean Dh (nm)	Mode Dh (nm)	Std. Dev. (nm)	Polydisp. (%)	Est. MW. (kDa)
1	12.55	12.86	1.97	15.73	282.7
2	247.09	250.51	42.01	17.00	Out of Rang

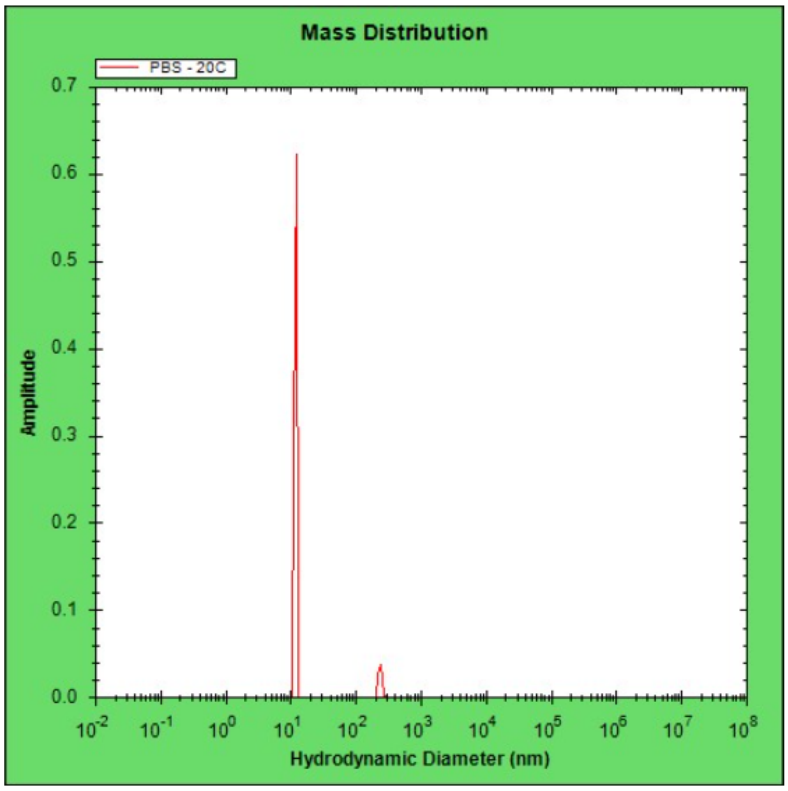

Figure 7: DLS imaging verifies completion of nanodisc formation. The mean mass distribution shows to be 12.55 nm which verifies the expected results of nanodisc diameter being 12 nm for an MSP-11 nanodisc.

Successful nanodisc formation verification using TEM

With the completion of TEM, nanodisc formation was verified showing a variation of sizes. This sample was not purified prior to imaging completion. The image shows a variation of size in nanodiscs which indicates that there may have been no complete initial circularization of MSP-11 prior to the insertion of bR (Figure 8).

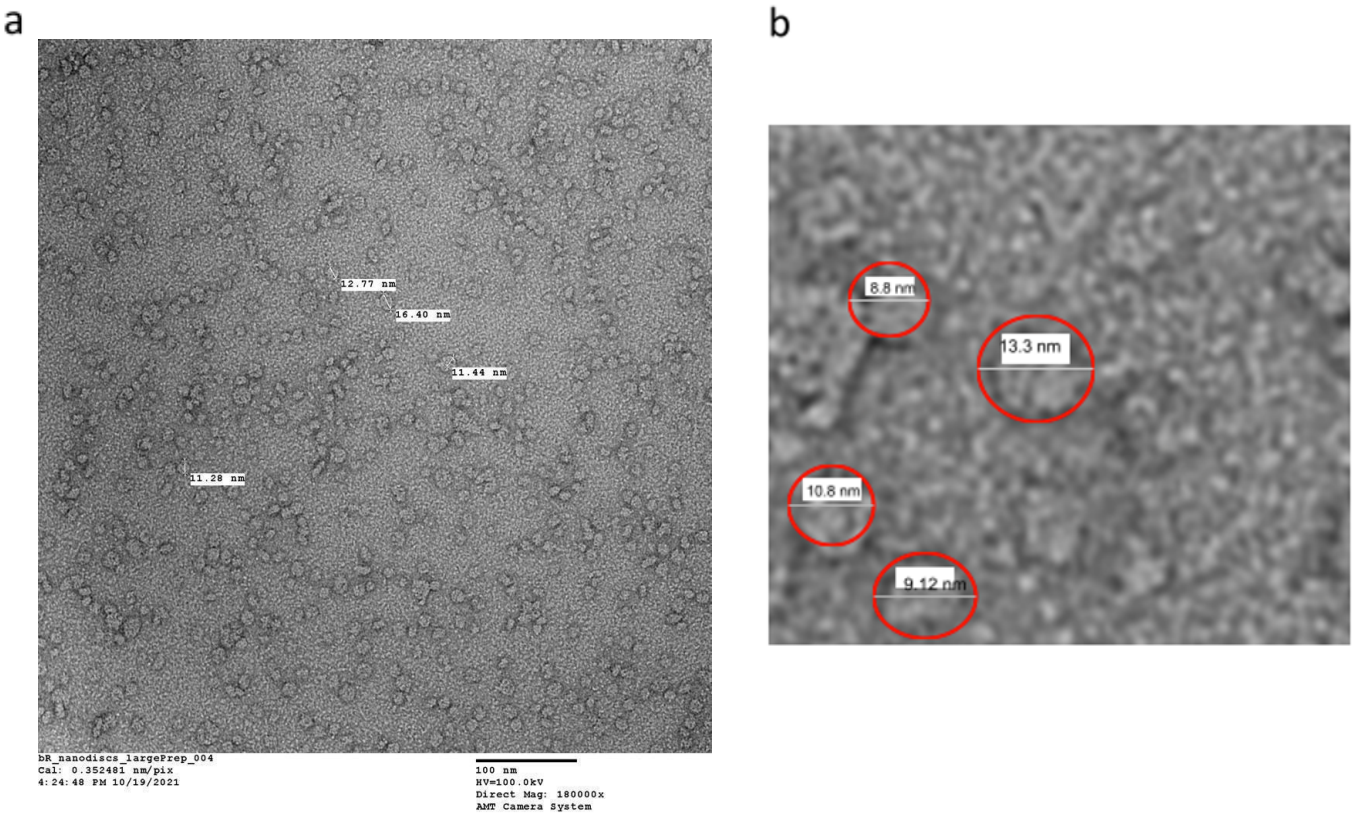

Figure 8: Verification bR-WT nanodiscs using TEM. (a) Preliminary image showing the presence of nanodiscs. (b-d) Zoomed in TEM image containing various sizes of nanodiscs.

Successful nanodisc formation verification with properly inserted bR-WT using FPLC

The results for the FPLC verify properly folded bR-WT within the nanodiscs in elution absorbance. The red line indicates absorption at 280 nm and the blue line shows absorption at 560 nm. The FPLC shows that when measuring at 280 nm, there is an increase in absorbance following ~5 mL of elution. This indicates the presence of protein aggregates and liposomes which naturally self-assemble. There is no signal in this area for 560 nm because only correctly folded bR will emit a signal. Within ~21 mL elution, there is a strong absorption spike and drop

of both 560 nm and 280 nm indicating the presence of MSP-11 and bR. Aspects of these results seem unusual which is due to the issues with the detection unit of the FPLC. Despite this, the FPLC results validate the presence of nanodiscs with properly folded bR because of the peak absorbance overlap for both 280 nm and 560 nm. The remaining bump in absorbance for 280 nm following the overlap could be unreacted MSP-11 within the solution (Figure 9).

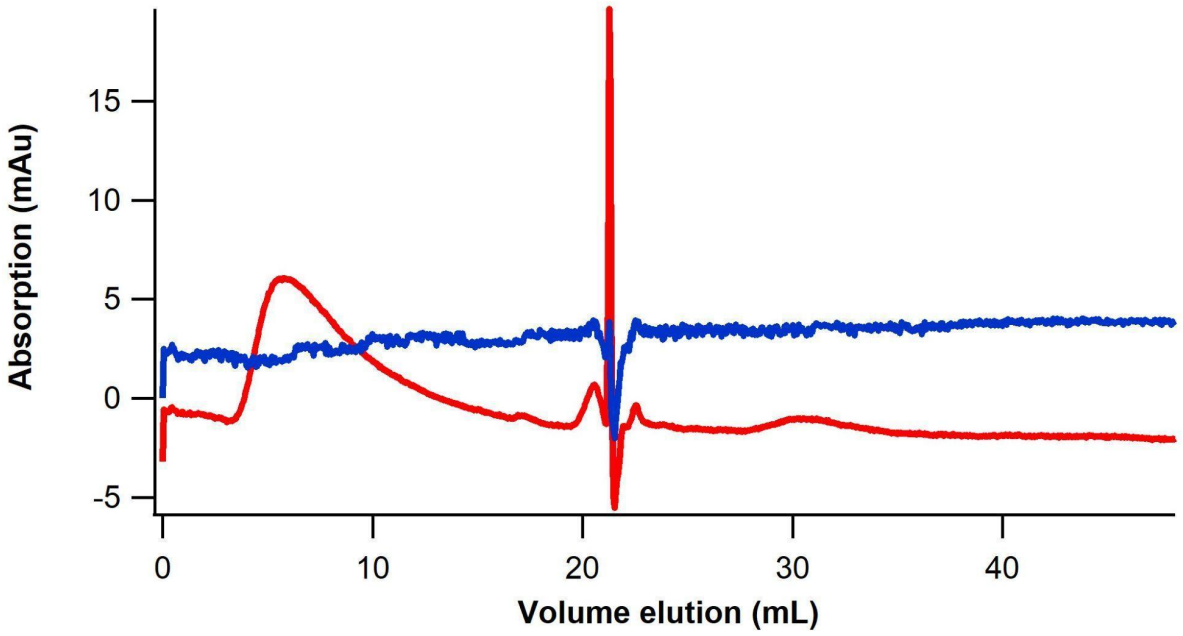

Figure 9: FPLC verifies properly folded bR-WT within nanodiscs in elution. Data analysis shows a peak at 560 nm and 280 nm absorption, indicating that bR within nanodiscs is folded correctly in the elution. Only correctly folded bR will absorb at 560 nm[1]. Red is 280 nm and Blue is 560 nm.

DBCO-PEG-maleimide reaction allowing for accurate site-specific attachment

DBCO-PEG-maleimide reaction protein gel electrophoresis shows the accurate completion of labeling. The gel shows bR to be present where expected at 27 kDa. The ladder that is present indicates that the C-Azide band contains a higher band which verifies that the reaction occurred (Figure 10).

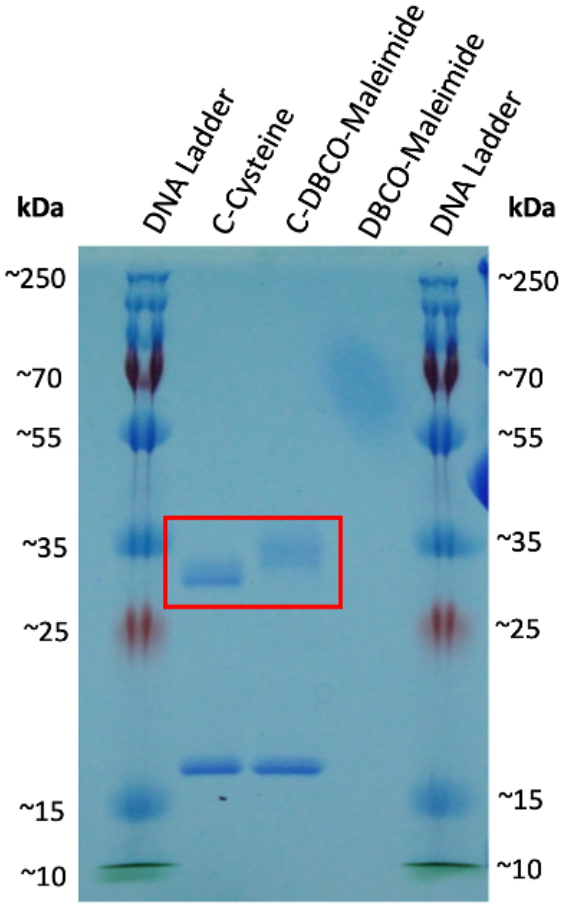

Figure 10: DBCO-PEG-maleimide reaction gel shows verification of completion allowing for accurate site-specific attachment to be completed. bR shows to have expected kDa of 27 which verifies successful labeling of DBCO-PEG-Maleimide which contains a higher kDa.

Aim Two:

AFM imaging of nanodisc formation containing c-terminal cysteine bR

To complete AFM imaging, the sample was moved from x to y with the cantilever tip moved across the surface. Nanodisc presence is verified within the images measured based on the deflection of the cantilever using Tapping Mode[13] Tapping Mode allows for a more gentle imaging of the sample without dragging molecules across the surface. Images show presence of nanodiscs, however the resolution of bR within the nanodiscs cannot be determined. Size variation remains consistent with the results from the TEM imaging (Figure 11).

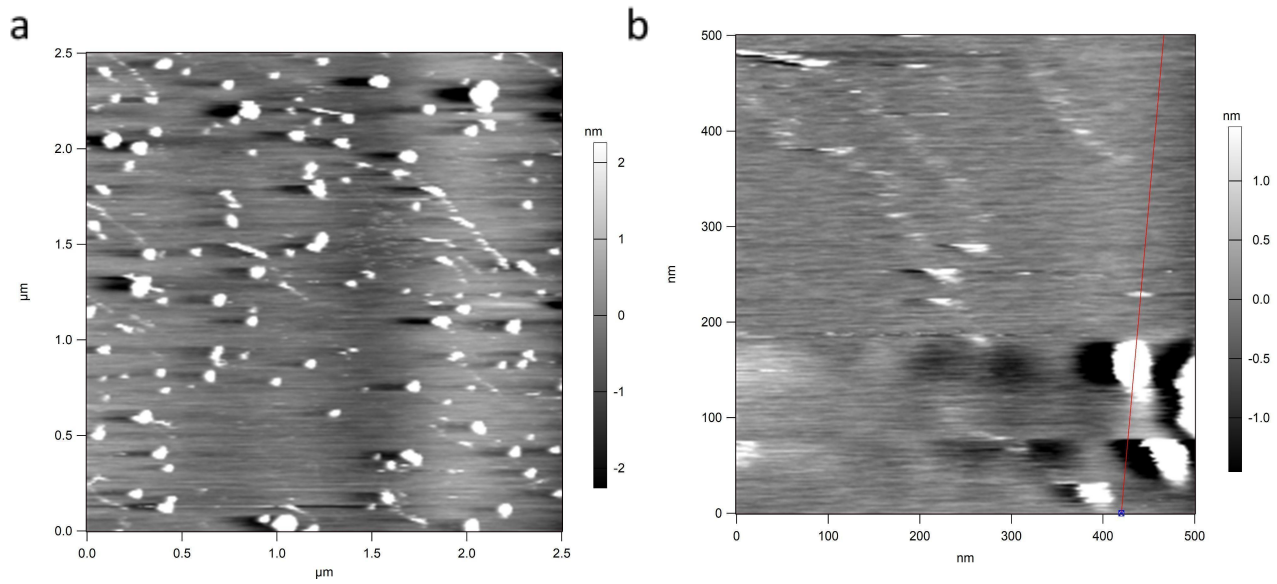

Figure 11: Representative atomic force spectroscopy imaging shows complete nanodisc formation and deposition. (a) The height of the nanodiscs is consistent with the expected height of the nanodiscs. There was not enough detail to resolve the bR. (d) Representation of bare mica patch surface with fewer nanodiscs.

C-terminal cysteine bR embedded nanodisc pulling experiment

To analyze the AFM pulling results, the data were fit using a worm-like chain model[30], with a fixed persistence length of 0.4 nm (Figure 12: b-d). Analysis was performed on data collected at 50 kHz that was smoothed to 5 kHz13. In the initial AFM- based SMFS attempt, we obtained 29 potentially successful pulls out of 1839, setting the hit rate as 1.5%. Ultimately, this is significantly higher than non-specific AFM pulling experiments[18]. These experiments were completed at a constant velocity of 1600 nm/s and 400 nm/s, with roughly an equal number of hits. By summing the change in contour length during the pulling, the length of the bR protein can be measured. The accepted bR membrane protein length is measured to be 70 nm[30]. With the representative trace, the length of the bR protein is measured to be 98.7 nm (Figure 12b). The additional trace showed the length of bR to be 77.1 nm (Figure 12c). This discrepancy could be due to improper folding of bR within the nanodisc or multiple bR proteins inserted into the membrane. Figure 12c shows a representation of an accurate bR trace from literature[17].

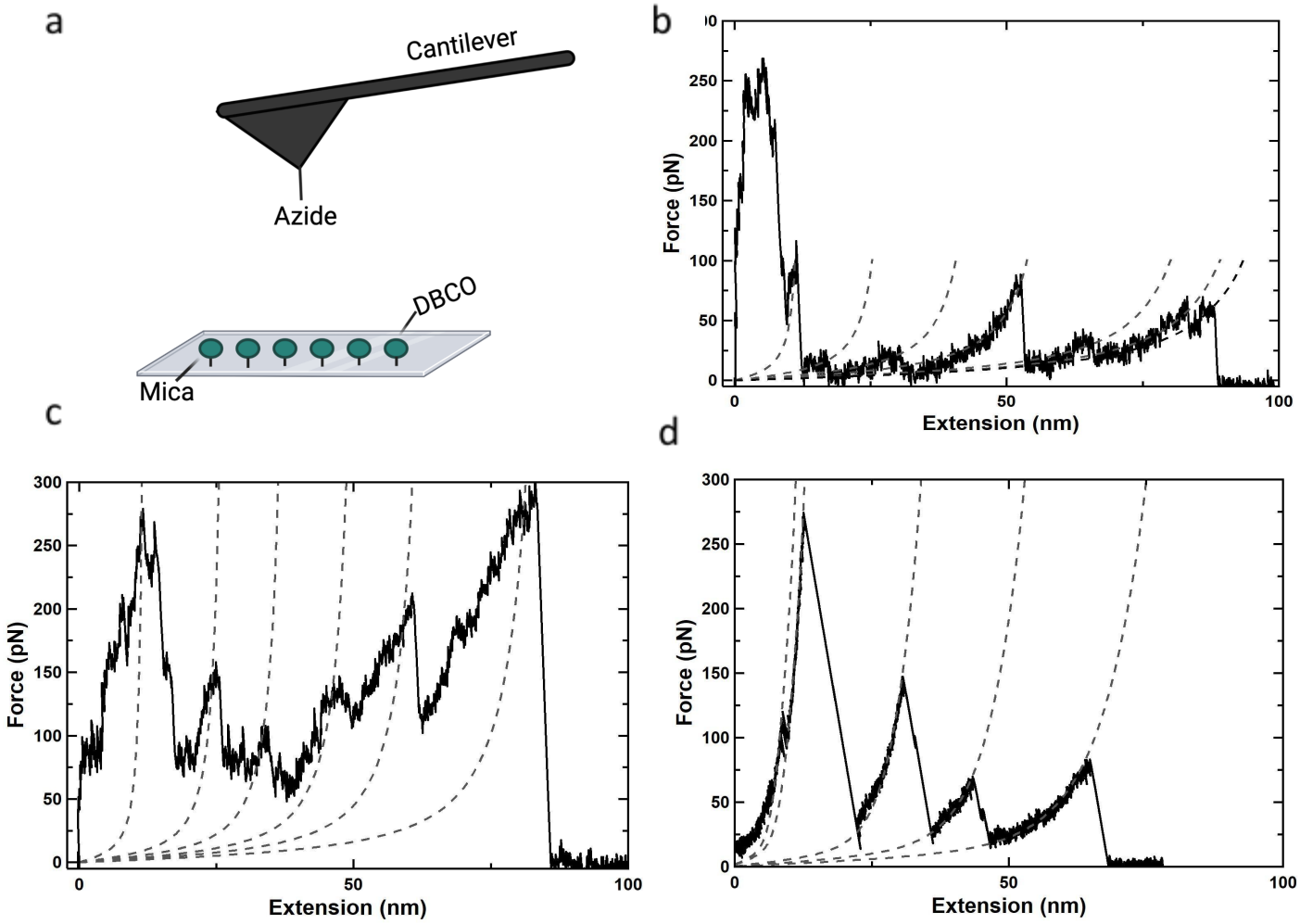

Figure 12: Representative dynamic force spectrum for bR c-terminal Cys bR in nanodisc technology. (a) Schematic of an experiment showing Azide-PEG-Silane labeled cantilever tip with DBCO-maleimide labeled nanodiscs. (b-c) Force extension curves show to have bR unfolding completed within nanodiscs. The segments of the force-extension curves between domain ruptures are fitted to worm-like chain models (dashed grey lines). (d) Representation of accurate bR trace utilizing AFM pulling observed in literature[19].

Table 1. (b) Representative trace of AFM-based SMFS on nanodiscs containing c-terminal cysteine bR.

Contour Length	Persistence Length	Contour Length Guess	Persistence Length Guess (M)	Rupture Force N	Loading Rate N/s	Velocity (nm/s)	Contour Length (nm)	Change in Contour Length	Rupture Force
$1.33E^{-8}$	$4.00E^{-10}$	$2.00E^{-8}$	$4.00E^{-10}$	$1.05E^{-10}$	1.09E-8	$4.00E^{-7}$	13.3	17.0	$1.05E^{+2}$
$3.03E^{-8}$	$4.00E^{-10}$	$2.26E^{-8}$	$4.00E^{-10}$	$1.37E^{-11}$	5.83	$4.00E^{-7}$	30.3	18.41	$1.37E^{+1}$
$4.87E^{-8}$	$4.00E^{-10}$	$3.86E^{-8}$	$4.00E^{-10}$	$2.37E^{-11}$	$2.73E^{-9}$	$4.00E^{-7}$	48.7	15.7	$2.37E^{+1}$
$6.44E^{-8}$	$4.00E^{-10}$	$7.50E^{-8}$	$4.00E^{-10}$	$8.16E^{-11}$	$3.01E^{-9}$	$4.00E^{-7}$	64.4	31.6	$8.16E^{+1}$
$9.60E^{-8}$	$4.00E^{-10}$	$9.92E^{-8}$	$4.00E^{-10}$	$3.26E^{-11}$	$4.87E^{-10}$	$4.00E^{-7}$	96.0	10.9	$3.26E^{+1}$
$1.07E^{-8}$	$4.00E^{-10}$	$1.04E^{-7}$	$4.00E^{-10}$	$5.67E^{-11}$	$1.26E^{-9}$	$4.00E^{-7}$	$1.07E^{+2}$	51.1	$5.67E^{+1}$
$1.12E^{-8}$	$4.00E^{-10}$	$1.09E^{-7}$	$4.00E^{-10}$	$5.92E^{-11}$	$7.50E^{-10}$	$4.00E^{-7}$	$1.12E^{+2}$		$5.92E^{+1}$

Total length: 98.7 nm

Table 2. (c) Additional trace of AFM-based SMFS on nanodiscs containing c-terminal cysteine bR.

Contour Length	Persistence Length	Contour Length Guess	Persistence Length Guess (M)	Rupture Force N	Loading Rate N/s	Velocity (nm/s)	Contour Length (nm)	Change in Contour Length	Rupture Force
$1.26E^{-8}$	$4.00E^{-10}$	$2.00E^{-8}$	$4.00E^{-10}$	$2.70E^{-10}$	$8.63E^{-9}$	$4.00E^{-7}$	$1.26E^{+1}$	15.5	$2.70E^{+2}$
$2.81E^{-8}$	$4.00E^{-10}$	$2.57E^{-8}$	$4.00E^{-10}$	$1.49E^{-10}$	$3.69E^{-9}$	$4.00E^{-7}$	$2.81E^{+1}$	11.9	$1.49E^{+2}$
$4.00E^{-8}$	$4.00E^{-10}$	$4.50E^{-8}$	$4.00E^{-10}$	$1.03E^{-10}$	$3.15E^{-9}$	$4.00E^{-7}$	$4.00E^{+1}$	13.7	$1.03E^{+2}$
$5.37E^{-8}$	$4.00E^{-10}$	$5.75E^{-8}$	$4.00E^{-10}$	$1.36E^{-10}$	$1.78E^{-9}$	$4.00E^{-7}$	$5.37E^{+1}$	13.3	$1.36E^{+2}$
$6.70E^{-8}$	$4.00E^{-10}$	$7.50E^{-8}$	$4.00E^{-10}$	$2.06E^{-10}$	$3.96E^{-9}$	$4.00E^{-7}$	$6.70E^{+1}$	22.7	$2.06E^{+2}$
$8.97E^{-8}$	$4.00E^{-10}$	$1.00E^{-7}$	$4.00E^{-10}$	$2.91E^{-10}$	$2.75E^{-9}$	$4.00E^{-7}$	$8.97E^{+1}$		$2.91E^{+2}$

Total length: 77.1 nm

Discussion and Future Directions

bR-WT and c-terminal cysteine bR yield following grow-up

Since the membrane protein that was selected to be embedded into nanodiscs was bR, we grew up a large batch of culture to work with nanodisc assembly initially. In order for the site-specific attachment to occur, the bR would need to be transformed to have a c-terminal cysteine allowing for covalent attachments with the cantilever. The yield for the transformed c-terminal cysteine bR was significantly lower than that of the wild-type bR which was anticipated.

Completion of nanodisc formation and verification of success

When completing nanodisc formation, the literature showed initial data with the increased yield of proper nanodisc circularization when completing circularization before completing the addition of membrane proteins. When the circularization reaction was completed, a protein gel was completed to verify the accuracy of the circularization of the Sortase-TEV which indicated that proper circularization occurred (Figure 6). The concentration of MSP-11 circularization was measured to be 14.4 μM at 560 nm absorption[1]. Due to this concentration, we expected that only ⅓ of the MSP-11 is correctly circularized. After nanodisc formation, the concentration was measured of bR at 560 nm absorption and 280 nm for MSP-11 concentration of both bR-WT and c-terminal cysteine bR[1]. The concentration of bR was measured at bR-WT (0.15 μM) and c-terminal cysteine bR (0.11 μM) using a NanoDrop. The absorption for MSP-11 concentration at 280 nm absorption was measured at bR-WT (3.3 μM) and c-terminal cysteine bR (2.8 μM) using a NanoDrop. These significantly low concentrations of bR compared to MSP-11 indicate that a majority of the bR is not properly folded within the nanodiscs. To verify

that nanodisc formation occurred, initial DLS imaging was completed with an expected diameter of 12 nm (Figure 13-15). Following imaging using TEM, it appears that there are a variety of sizes of nanodiscs which was not expected due to the expectation of homodisperse formation where there is a relatively large range of sizes (Figure 8). This verifies that there may be the presence of more than one bR within the nanodisc when assembled, which will be greatly resolved when purification occurs for this sample using FPLC.

Verification of the presence of properly folded bR with the nanodiscs

The FPLC that was completed was done on bR-WT to allow for proper purification of the sample (Figure 9). When looking at the results of the FPLC, the trace does not have very good data which may be attributed to various errors. The early peak that we see in the 280 nm UV signal is due to the aggregates and other large substrates that weren't incorporated into the nanodisc (Figure 9). During the process of FPLC, the UV detector was failing which may have caused this poor trace. The trace observed also shows it could be due to improperly folded bR within the nanodiscs which was observed in AFM imaging and pulling (Figure 12: b-d).

AFM initial representative imaging of nanodiscs

The final nanodisc preparation was completed utilizing c-terminal cysteine bR for AFM pulling and imaging experiments. With initial imaging, there was a significant amount of movement that the nanodiscs had on the surface (Figure 11: b-d). Due to nanodisc imaging indicating movement, the sample was saturated with ~10 mM Mg^{2+} in-situ to increase the electrostatics and adhesion to the surface. These results were not included within this thesis due to the lack of success the addition of Mg^{2+} had. These experiments indicated that there was an

issue with the 2-part epoxy used to secure the mica disc to the steel specimen disc leading to sliding when the cantilever met the sample. With future experimentation, we can complete imaging that has secure discs which would provide much cleaner data. This data would greatly be purified with the proper adhesion of the discs together.

AFM-based site-specific SMFS on c-terminal cysteine bR nanodiscs

Following initial force spectroscopy pulling on c-terminal cysteine bR, preliminary data shows that the representative traces were unable to return to baseline in between attachments. A decrease in surface nanodisc density pulling would allow for more accurate results, decreasing the amount of interference between attachments. Another possible way to gather cleaner data would be to make a surface with non-stick heterobifunctional PEG, which allows for specific places to contain samples within the surface. There is a vast variety of types of heterobifunctional PEG that have been verified and would be performed for additional experiments using AFM. Another option would be to add a tag to the MSP-11 changing a nonspecific attachment to a specific attachment allowing for the MSP-11 to be selectively deposited onto the surface for experimentation.

One potential technical drawback general to site-specific attachment when completing force spectroscopy is that in the best case, there are 10-30 attachments before the tip is dysfunctional (Figure 12: b-c). This is due to the fact the attachments that are completed are covalent interactions, and thus cannot be reversed. Moving to a non-covalent interaction would allow for increased data collection. The data collected gave us the proof of principle allowing for future experimentation utilizing non-covalent interactions.

My senior thesis demonstrates the optimization of nanodisc formation using a TEV and Sortase covalent circularization of 12 nm MSP-11. Along with this, successful c-terminal cysteine bR insertion into a nanodisc native lipid membrane was completed. Additionally, we completed a successful representative trace utilizing AFM imaging and force spectroscopy to further characterize membrane protein dynamics. Overall, this thesis validates the ability to optimize nanodiscs formation using bR labeled with a c-terminal cysteine and the ability to utilize AFM to further examine and deduce different membrane protein dynamics in their native lipid environment.

Acknowledgments

Thank you to Dr. Thomas Perkins for the opportunity to complete this research within his laboratory and for the constant support. I worked directly with Dr. Marc-Andre LeBlanc who without this project would be impossible to complete. I appreciate the opportunity to work with him and the continual assistance and incredibly vast knowledge. Thank you to Lyle Uyetake for the help with working with bacteria grow-up and transformation patiently. Finally, thank you to Dr. David Jacobson for all the support with AFM imaging that I couldn't have completed without him.

Thank you to all of the members of Perkins lab and JILA for their acceptance and willingness to help me through this project. I am grateful for the opportunity to work with such intelligent people who supported me through this learning experience.

Supplementary Information

Table 3. bR-WT sequence compared to c-terminal cysteine bR sequence

Translated bR before cleavage MLELLPTAVEGVSQAQITGRPEWIWLALGTALMGLGTLYFLVKGMGVSDP DAKKFYAITTLVPAIAFTMYLSMLLGYGLTMVPFGGEQNPIYWARYADWL FTTPLLLLDLALLVDADQGTILALVGADGIMIGTGLVGALTKVYSYRFVW WAISTAAMLYILYVLFFGFTSKAESMRPEVASTFKVLRNVTVVLWSAYPVV WLIGSEGAGIVPLNIETLLFMVLDVSAKVGFGLILLRSRAIFGEAEAPEPSA GDGAAATSD*
Mature bR-wt (the sequence that we use): QAQITGRPEWIWLALGTALMGLGTLYFLVKGMGVSDPDAKKFYAITTLVP AIAFTMYLSMLLGYGLTMVPFGGEQNPIYWARYADWLFTTPLLLLDLALL VDADQGTILALVGADGIMIGTGLVGALTKVYSYRFVWWAISTAAMLYILY VLFFGFTSKAESMRPEVASTFKVLRNVTVVLWSAYPVVWLIGSEGAGIVPL NIETLLFMVLDVSAKVGFGLILLRSRAIFGEAEAPEPSAGDGAAATS
c-terminal cys bR QAQITGRPEWIWLALGTALMGLGTLYFLVKGMGVSDPDAKKFYAITTLVP AIAFTMYLSMLLGYGLTMVPFGGEQNPIYWARYADWLFTTPLLLLDLALL VDADQGTILALVGADGIMIGTGLVGALTKVYSYRFVWWAISTAAMLYILY VLFFGFTSKAESMRPEVASTFKVLRNVTVVLWSAYPVVWLIGSEGAGIVPL NIETLLFMVLDVSAKVGFGLILLRSRAIFGEAEAPEPSAGDGAAATC

Table 4. Initial bR-WT nanodisc formation

Sample Number	bR (µL) 25 µm	NaCl (µL) 2.5 M	Tris (µL) - buffer, 0.5 mM EDTA	Triton X-100 (µL)	MSP-11 (µL)	H_2O µL (UltraPure)	Total Volume (µL)
1	7.1	25	1.25	1.18	15.47	0	50
2	7.1	25	1.25	1.18	9.7	5.8	50
3	7.1	25	1.25	0.6	9.7	0.6	50
4	7.1	25	1.25	2.36	9.7	4.62	50
5	7.1	30.8	1.25	1.18	9.7	0	50
6	4.25	25	1.25	1.18	15.47	2.85	50

Table 5. Variation for optimization of bR-WT nanodisc formation

Sample Number	bR (µL)	NaCl (µL) 2.5 M	Tris (µL) - buffer, 0.5 mM EDTA	Triton X-100 (µL)	MSP-11 (µL)	H_2O µL (UltraPure)	Total Volume (µL)	bR:MSP, Triton Concentration
1	7	35.54	1.25	0.59	5.62	0	50	Triton 5 mM
2	7	34.95	1.25	1.18	5.62	0	50	Triton 10 mM
3	7	34.95	1.25	1.18	5.62	0	50	Triton 10 mM; increase biobeads
4	7	33.79	1.25	2.34	5.62	0	50	Triton 20 mM
5	7	40.57	1.25	1.18	0	0	50	Negative control MSP-11; 10 mM Triton

Table 6. Large bR-WT preparation for imaging

Sample Number	bR (µL)	NaCl (µL) 2.5 M	Tris (µL) - buffer, 0.5 mM EDTA	Triton X-100 (µL)	MSP-11 (µL)	H_2O µL (UltraPure)	Total Volume (µL)	bR:MSP, Triton concentration
3	35.43	174.75	6.25	5.9	28.1	0	250	750 micoL of biobeads

Table 7. Final bR-WT and c-terminal cysteine bR preparation for AFM SMFS and imaging

Sample Number	bR (µL)	NaCl (µL) 2.5 M	Tris (µL) - buffer, 0.5 mM EDTA	Triton X-100 (µL)	MSP-11 (µL)	H_2O µL (UltraPure)	Total Volume (µL)	bR:MSP, Triton concentration
3 bR (cCys)	50	246.61	8.82	8.33	18.78			999
bR-WT	50	246.64	8.82	8.43	20.05		333.94	1002

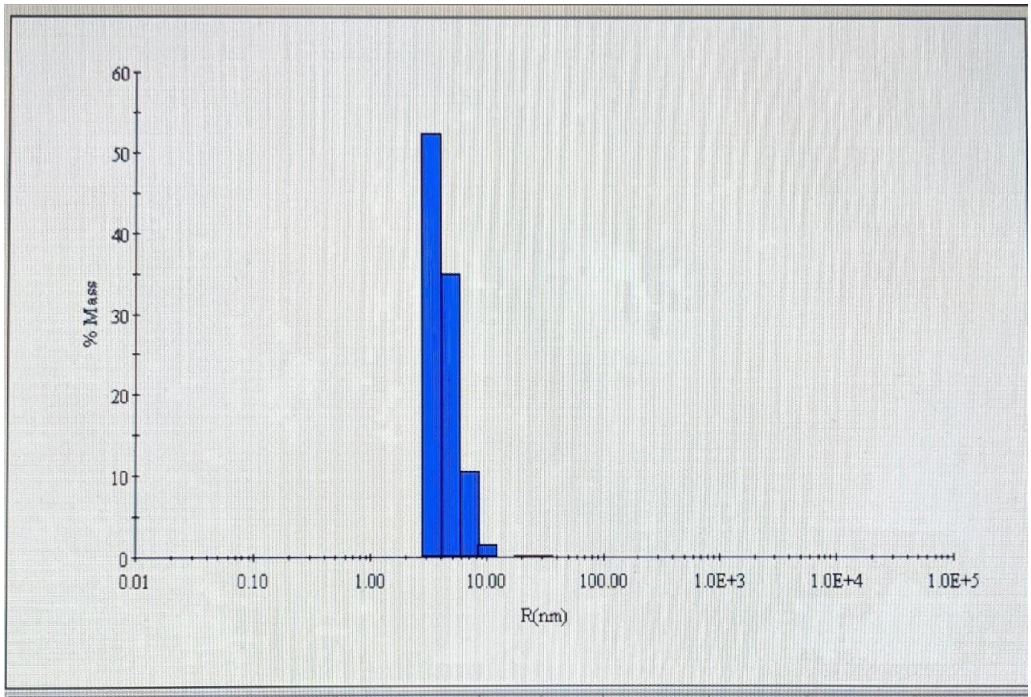

Item	R	%Pd	MW-R	%Int	%Mass	D	Diam	Pd Index
	(nm)		(kDa)			(cm²/s)	(nm)	
Peak 1	4.42119	31.0236	109	21.3	99.6	4.888e-007	8.8	9.625e-002
Peak 2	33.7174	39.3713	12649	42.1	0.4	6.410e-008	67.4	1.550e-001
Peak 3	3148.68	32.4862	515348000	36.6	0.0	6.864e-010	6297.4	1.055e-001

Figure 13: Initial dynamic light scattering data of bR-WT nanodisc prep with 5 mM Triton X-100. The image shows particle size smaller than expected.

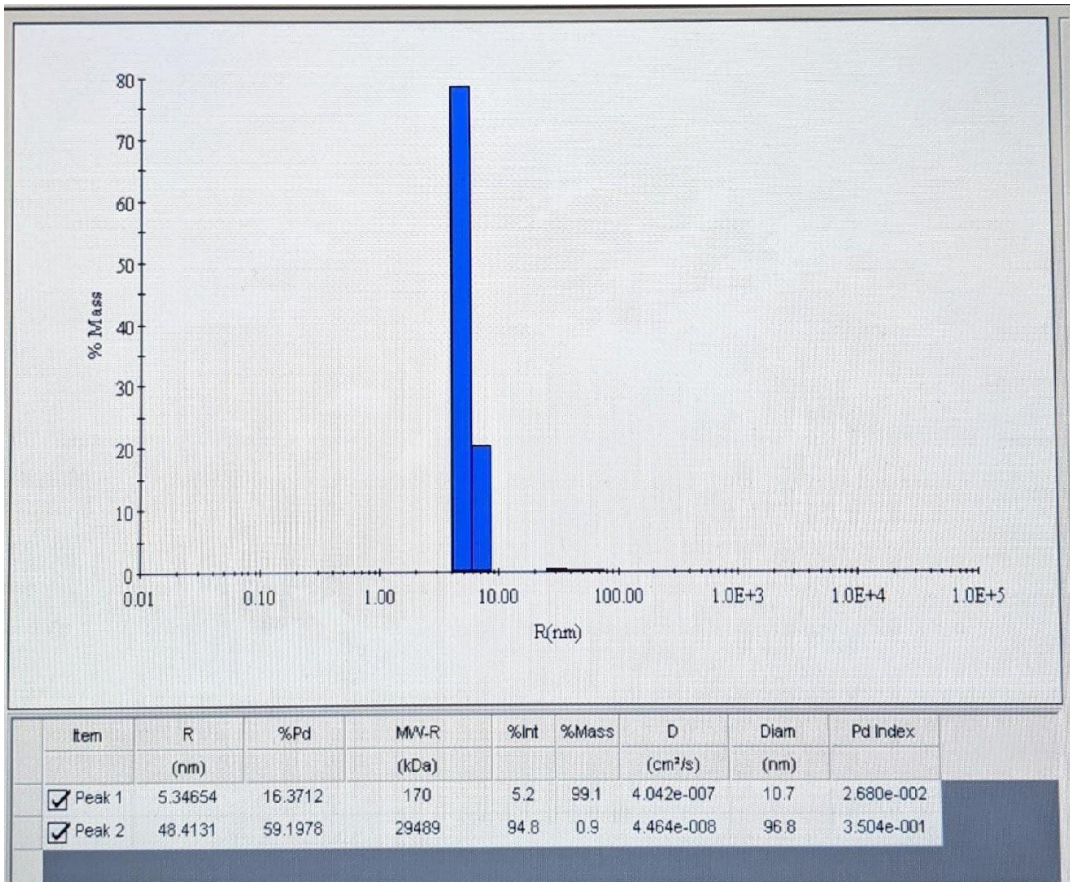

Item	R	%Pd	MW-R	%Int	%Mass	D	Diam	Pd Index
	(nm)		(kDa)			(cm²/s)	(nm)	
Peak 1	5.34654	16.3712	170	5.2	99.1	4.042e-007	10.7	2.680e-002
Peak 2	48.4131	59.1978	29489	94.8	0.9	4.464e-008	96.8	3.504e-001

Figure 14: Initial dynamic light scattering data of bR-WT nanodisc prep with 20 mM Triton X-100. The image shows particle size smaller than expected for MSP-11 (12nm).

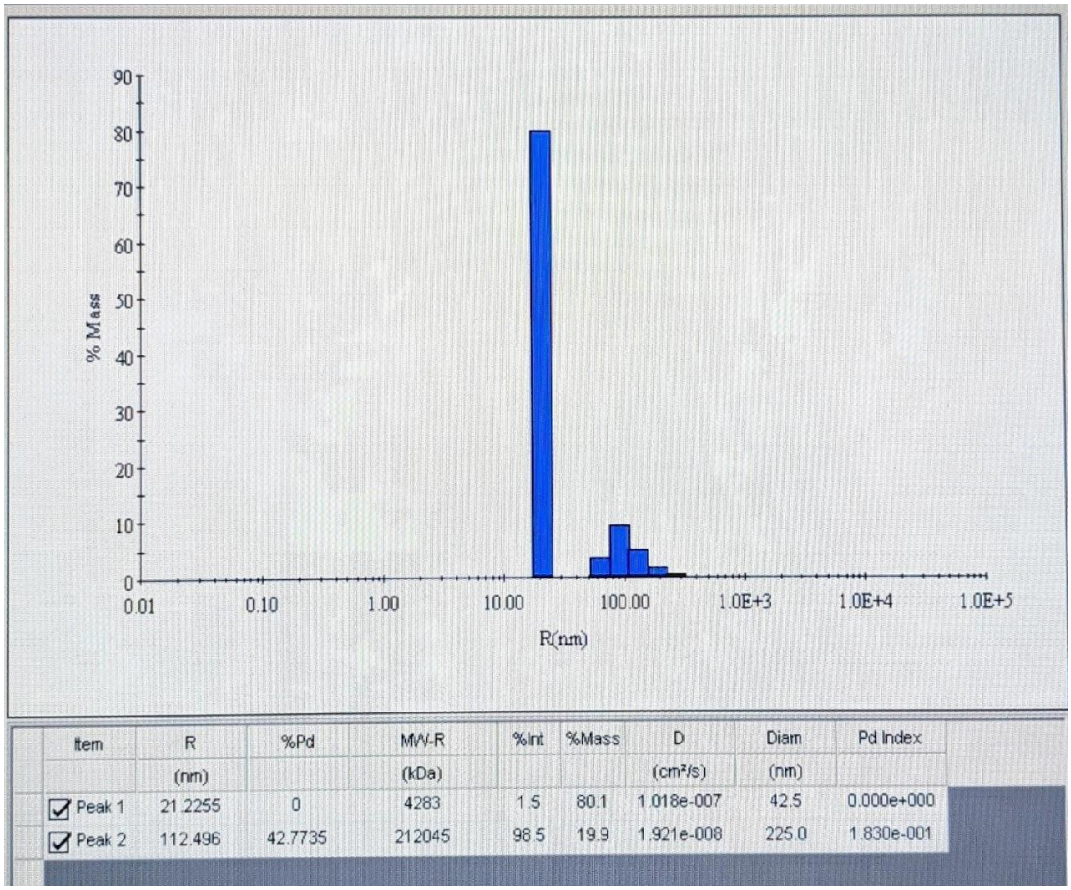

Item	R (nm)	%Pd	MW-R (kDa)	%Int	%Mass	D (cm²/s)	Diam (nm)	Pd Index
Peak 1	21.2255	0	4283	1.5	80.1	1.018e-007	42.5	0.000e+000
Peak 2	112.496	42.7735	212045	98.5	19.9	1.921e-008	225.0	1.830e-001

Figure 15: Initial dynamic light scattering data of bR-WT nanodisc prep with 2X NaCl. The image shows particle size closer to the expected MSP-11 size at 12 nm. There is a presence of much larger particles which could be aggregates of unfolded bR within the sample.

References

1.Maeda, A., Takeuchi, Y. & Yoshizawa, T. Absorption spectral properties of acetylated bacteriorhodopsin in purple membrane depending on pH. Biochemistry 21, 4479–4483 (1982).

2.Zhang, B. et al. An easy-to-use site-directed mutagenesis method with a designed restriction site for convenient and reliable mutant screening*. J Zhejiang Univ Sci B 10, 479–482 (2009).

3.Archive of 'Protein Science : A Publication of the Protein Society'. - PMC. https://www.ncbi.nlm.nih.gov/pmc/journals/507/.

4.Hagn, F., Nasr, M. L. & Wagner, G. Assembly of phospholipid nanodiscs of controlled size for structural studies of membrane proteins by NMR. Nat Protoc 13, 79–98 (2018).

5.Atomic Force Microscopy. Nanoscience Instruments https://www.nanoscience.com/techniques/atomic-force-microscopy/.

6.Lanyi, J. K. Bacteriorhodopsin as a model for proton pumps. Nature 375, 461–463 (1995).

7.Chemical Analysis, Life Sciences, and Diagnostics | Agilent. https://www.agilent.com/?gclid=CjwKCAjwloCSBhAeEiwA3hVo_aJ6pir3OTwWbtiJcCSSETzVOhZTtT7sXlt89YaCkvHRMluRMZNOshoC7FYQAvD_BwE&gclsrc=aw.ds.

8.Johansen, N. T. et al. Circularized and solubility-enhanced MSPs facilitate simple and high-yield production of stable nanodiscs for studies of membrane proteins in solution. FEBS J 286, 1734–1751 (2019).

9.Eeftens, J. M., van der Torre, J., Burnham, D. R. & Dekker, C. Copper-free click chemistry for attachment of biomolecules in magnetic tweezers. BMC Biophys 8, 9 (2015).

10.Kolberg, A., Wenzel, C., Hugel, T., Gallei, M. & Balzer, B. N. Covalent Attachment of Single Molecules for AFM-based Force Spectroscopy. JoVE (Journal of Visualized Experiments) e60934 (2020) doi:10.3791/60934.

11.Gruber, H. J. General information on the functionalization of atomic force microscopy (AFM) tips via long, flexible polyethylene glycol (PEG) chains. 14.

12.Yeh, V. et al. Highly Efficient Transfer of 7TM Membrane Protein from Native Membrane to Covalently Circularized Nanodisc. Sci Rep 8, 13501 (2018).

13.Ando, T. High-speed atomic force microscopy coming of age. Nanotechnology 23, 062001 (2012).

14.Li, M., Dang, D., Liu, L., Xi, N. & Wang, Y. Imaging and Force Recognition of Single Molecular Behaviors Using Atomic Force Microscopy. Sensors (Basel) 17, 200 (2017).
15.Lyubchenko, Y. L., Shlyakhtenko, L. S. & Ando, T. Imaging of nucleic acids with atomic force microscopy. Methods 54, 274–283 (2011).
16.large insertions : two simple steps using quikchange ® ii site-directed mutagenesis kits. https://www.semanticscholar.org/paper/large-insertions-%3A-two-simple-steps-using-%C2%AE-ii-kits/7d87dea4e4ba2558e00903c47bb27cfdb1ac706d (2007).
17.Cournia, Z. et al. Membrane Protein Structure, Function and Dynamics: A Perspective from Experiments and Theory. J Membr Biol 248, 611–640 (2015).
18.Seddon, A. M., Curnow, P. & Booth, P. J. Membrane proteins, lipids and detergents: not just a soap opera. Biochimica et Biophysica Acta (BBA) - Biomembranes 1666, 105–117 (2004).
19.Jacobson, D. R., Uyetake, L. & Perkins, T. T. Membrane-Protein Unfolding Intermediates Detected with Enhanced Precision Using a Zigzag Force Ramp. Biophysical Journal 118, 667–675 (2020).
20.Membranes in Biology & Medicine : Models to Medicine Center : UMass Amherst. https://www.umass.edu/m2m/research-themes/membranes-biology-medicine.
21.Molecular dynamics simulations of lipid nanodiscs. https://www.ncbi.nlm.nih.gov/pmc/articles/PMC6218321/.
22.Mutagenesis Kits | Agilent. https://www.agilent.com/en/product/mutagenesis-cloning/mutagenesis-kits.
23.Denisov, I. G. & Sligar, S. G. Nanodiscs for structural and functional studies of membrane proteins. Nat Struct Mol Biol 23, 481–486 (2016).
24.Denisov, I. G. & Sligar, S. G. NANODISCS IN MEMBRANE BIOCHEMISTRY AND BIOPHYSICS. Chem Rev 117, 4669–4713 (2017).
25.Li, M., Liu, L., Xi, N. & Wang, Y. Progress in measuring biophysical properties of membrane proteins with AFM single-molecule force spectroscopy. Chin. Sci. Bull. 59, 2717–2725 (2014).
26.Walder, R. et al. Rapid Characterization of a Mechanically Labile α-helical Protein Enabled by Efficient Site-Specific Bioconjugation. J Am Chem Soc 139, 9867–9875 (2017).
27.Rouck, J., Krapf, J., Roy, J., Huff, H. & Das, A. Recent Advances in Nanodisc Technology for Membrane Proteins Studies (2012–2017). FEBS Lett 591, 2057–2088 (2017).

28.Ritchie, T. K. et al. Reconstitution of Membrane Proteins in Phospholipid Bilayer Nanodiscs. Methods Enzymol 464, 211–231 (2009).
29.Zocher, M. et al. Single-Molecule Force Spectroscopy from Nanodiscs: An Assay to Quantify Folding, Stability, and Interactions of Native Membrane Proteins. ACS Nano 6, 961–971 (2012).
30.Müller, D. J. et al. Stability of Bacteriorhodopsin α-Helices and Loops Analyzed by Single-Molecule Force Spectroscopy. Biophysical Journal 83, 3578–3588 (2002).